



## Research Article

# Ionotropic Gelation Synthesis of Chitosan-Alginate Nanodisks for Delivery System and *In Vitro* Assessment of Prostate Cancer Cytotoxicity

David Patiño-Ruiz <sup>1</sup>, Leandro Marrugo,<sup>2</sup> Niradiz Reyes,<sup>3</sup> María Acevedo-Morantes,<sup>1,2</sup> and Adriana Herrera <sup>1,2</sup>

<sup>1</sup>Doctorate in Engineering Program, Nanomaterials and Computer Aided Process Engineering Research Group, Universidad de Cartagena, Cartagena, Colombia

<sup>2</sup>Chemical Engineering Program, Nanomaterials and Computer Aided Process Engineering Research Group, Universidad de Cartagena, Cartagena, Colombia

<sup>3</sup>Medicine Program, Universidad de Cartagena, Cartagena, Colombia

Correspondence should be addressed to Adriana Herrera; [aherrerab2@unicartagena.edu.co](mailto:aherrerab2@unicartagena.edu.co)

Received 3 August 2019; Revised 26 November 2019; Accepted 2 December 2019; Published 3 January 2020

Guest Editor: Di Li

Copyright © 2020 David Patiño-Ruiz et al. This is an open access article distributed under the Creative Commons Attribution License, which permits unrestricted use, distribution, and reproduction in any medium, provided the original work is properly cited.

We report on the synthesis of chitosan-alginate nanodisks (Cs-Al NDs) using a simple approach consisting of the ionotropic gelation method. Sodium tripolyphosphate (STPP) was used as crosslinking agent to promote the electrostatic interaction between amine groups the chitosan and hydroxyl and carboxyl groups of alginate. Scanning electron microscopy (SEM) images provided direct evidence of the morphology of the nanodisks where agglomeration was observed due to the electrostatic interaction between the functional groups. Furthermore, dynamic light scattering (DLS) showed that the hydrodynamic size of the Cs-Al NDs was 227 nm and 152 nm in pH 1.2 and pH 7.4, respectively, which is in agreement with the information observed in the SEM images. The chemical structure is presented mainly the amine and carboxyl groups due to the presence of chitosan and alginate in the nanodisks, respectively, which allow the electrostatic interaction through N-H linkages. According to the X-ray diffraction, we found that the Cs-Al NDs exhibited the typical structure of chitosan and alginate, which lead the formation of polyelectrolyte complexes. We also evaluated the encapsulation of amoxicillin in the nanodisk, obtaining a loading efficiency of 74.98%, as well as a maximum *in vitro* release amount of 63.2 and 52.3% at pH 1.2 and 7.4, respectively. Finally, the cytotoxicity effect of the Cs-Al nanodisks was performed in human prostatic epithelial PWR-1E and Caucasian prostate adenocarcinoma PC-3 cell lines, in which the cell viability was above 80% indicating low inhibition and determining the Cs-Al NDs as a promising technology for controlled delivery systems.

## 1. Introduction

Recently, natural polymers such as polysaccharides have been widely explored for the synthesis of nanomaterials applied to multiple applications, especially in the biomedical and pharmaceutical fields [1, 2]. Polysaccharides such as chitosan and alginate are abundant and can be found easily in the environment and possess excellent physico-chemical and biological properties such as biocompatibility, biodegradability, and low toxicity, which demonstrate

that these biopolymers are suitable for sustained and controlled drug delivery systems [3–5]. These biopolymers are catalogued as Generally Regarded as Safe (GRAS) by the Food and Drug Administration (FDA), allowing their use for drug delivery systems [6].

Chitosan is a linear and cationic biopolymer derived from chitin after a deacetylation process and consisted of  $\beta$  (1-4) linked 2-acetamido-2-deoxy- $\beta$ -D-glucopyranose and 2-amino-2-deoxy- $\beta$ -D-glucopyranose structures, offering abundant amine ( $-\text{NH}_2$ ) functional groups for better

adsorption capacity and environmental adaptability [1, 7, 8]. On the other hand, alginate is an anionic polymer derived from seaweeds and is chemically structured of (1,4) linked  $\beta$ -D-mannuronic and  $\alpha$ -L-guluronic acid moieties, in which the hydroxyl (-OH) and carboxyl (-COOH) functional groups enhance the availability and stability in acidic environments, offering a potential application for encapsulation and controlled release of drugs [9–11].

The amine and carboxyl groups of chitosan and alginate, respectively, can promote through an ionotropic gelation technique a rapid electrostatic interaction leading the formation of a polyelectrolyte complex nanocomposite widely used for wound dressing, tissue engineering, and drug delivery [12–14]. Ionotropic gelation consists of the crosslink of both biopolymers in the presence of polyvalent ion compounds such as sodium tripolyphosphate (STPP); however, the polycationic and polyanionic nature of the biopolymers may form a polyelectrolyte complex in aqueous solution spontaneously [12, 15]. Therefore, the combination of both biopolymers is shown to be more effective than chitosan or alginate separately, improving the binding performance and stability in acidic and basic environments, which enables more controlled delivery and release of drugs according to the external stimuli, and may be also extended to other characteristics of the environment such as temperature and ion strength [16, 17].

We hereby report the synthesis of chitosan-alginate nanodisks (Cs-Al NDs) using the ionotropic gelation technique, in which STPP was used as the highly charged agent to promote the strong electrostatic interaction between the functional groups of both biopolymers. In this study, scanning electron microscopy (SEM), dynamic light scattering (DLS), Fourier-transform infrared spectroscopy (FTIR), and X-ray diffraction (XRD) were performed to obtain morphological and physical information, respectively. We also evaluate the encapsulation efficiency and *in vitro* release capacity of the Cs-Al NDs in acidic and basic environments, using amoxicillin as the model drug. Finally, we assessed the cytotoxicity effects of the Cs-Al NDs on the cell viability of human prostatic epithelial PWR-1E and Caucasian prostate adenocarcinoma PC-3 cell lines.

## 2. Materials and Methods

**2.1. Materials.** Chitosan (85% deacetylation), sodium tripolyphosphate (STPP), and acetic acid were purchased from Alfa Aesar, and sodium alginate was from Danisco. Hydrochloric acid (HCl), potassium phosphate ( $K_3PO_4$ ), sodium hydroxide (NaOH), and potassium chloride (KCl) were supplied from Panreac. Amoxicillin was acquired from Genfar. Human cell lines PC-3 and PWR-1E were obtained from American Type Culture Collection (ATCC). Fetal bovine serum, penicillin-streptomycin, keratinocyte culture, bovine pituitary extract, and EGF recombinant human protein were supplied from Thermo Fisher Scientific. Phosphate-buffered saline (PBS), trypan blue, phenazine ethosulfate (PES), and (3-(4,5-dimethylthiazol-2-yl)-5-(3-carboxymethoxyphenyl)-2-(4-sulfophenyl)-2H-tetrazolium) MTS were purchased from Sigma-Aldrich. CellTiter 96®

Aqueous One Solution Cell Proliferation Kit was acquired from Promega.

**2.2. Synthesis of Chitosan-Alginate Nanodisks (Cs-Al NDs).** The Cs-Al NDs were prepared by ionotropic gelation of chitosan and sodium alginate using STPP as a highly charged agent [18]. Chitosan (2.25 mg/mL) was added in acetic acid solution at 1% v/v under magnetic stirring at 700 rpm until the biopolymer was dissolved completely. Then, sodium alginate (0.5 mg/mL) and STPP (1 mg/mL) solutions were prepared in distilled water and mixed to perform the chitosan crosslinking. Gelation was carried out by dropwise addition of the sodium alginate/STPP solution into the chitosan gel following a 3:1 v/v ratio under magnetic stirring at 700 rpm for 10 min. Finally, the suspension was centrifuged to precipitate the Cs-Al NDs at 5500 rpm for 15 min, and then the supernatant containing unreacted polymer was removed gently using a pipette. The as-synthesized Cs-Al NDs were washed several times with distilled water and then lyophilized to obtain the final product.

**2.3. Characterization.** The surface morphology and shape of the lyophilized Cs-Al NDs were observed using the scanning electron microscopy (SEM) technique in a high-performance JEOL JSM 6490 LV equipment with a high resolution of 3.0 nm and low vacuum mode. The Cs-Al NDs for imaging were drop casted onto gold coat in a sputter coater and left to dry at room temperature. The hydrodynamic size and particle size distribution were determined using a dynamic light scattering (DLS) Horiba LB-550 equipment. Functional groups were determined using a NICOLET 6700 FT-IR (Thermo Scientific) equipment with a wavelength between 400 and 4000  $cm^{-1}$ . X-ray diffraction (XRD) was carried out with the aim to obtain crystalline information using an XPert PANalytical Empyrean Series II with a  $2\theta$  range from 5 to 80°. The Cs-Al NDs were dispersed in 2 buffer solutions at pH 1.2 and 7.4 using an ultrasound bath and then analyzed in quintuplicate. UV-Vis spectrophotometry spectra to determine the encapsulation efficiency and release of amoxicillin at pH 1.2 and 7.4 were collected using an UV-2650 spectrometer.

**2.4. Encapsulation Efficiency of Amoxicillin.** Amoxicillin was used as a model drug for encapsulation in Cs-Al NDs. Following the process for nanodisk preparation, amoxicillin (0.1 mg/mL) was added to the STPP solution before crosslinking with chitosan. The gelation process was the same as mentioned in a previous step for Cs-Al NDs synthesis. The encapsulation efficiency (EE) of amoxicillin was calculated using the supernatant obtained after centrifugation, in which an UV-2650 UV-Vis spectrophotometer was used to measure the absorbance at 247 nm. Calibration curves allowed to quantify the amount of free amoxicillin in the supernatant and then to determine EE% in triplicate according to

$$EE(\%) = \left( \frac{\text{Total content} - \text{free content}}{\text{Total content}} \right) \times 100. \quad (1)$$

**2.5. In Vitro Release of Amoxicillin.** A study of amoxicillin releases was performed using PBS solutions at pH 1.2 and 7.4, in order to evaluate the controlled delivery of the drug and the stability of the Cs-Al NDs in acidic and basic mediums, respectively. The PBS at pH 1.2 was prepared using 50 mL of KCl (0.2 M) and 85 mL of HCl (0.2 M) solutions, and in parallel, the PBS at pH 7.4 was obtained mixing 100 mL of  $K_3PO_4$  (0.1 M) and 78.2 mL of NaOH (0.1 M). Then, 30 mg of amoxicillin loaded Cs-Al NDs was dispersed in 120 mL of each PBS solution and placed in an incubator shaker under 150 rpm at 37°C for a total period of 8 h. Aliquots of 5 mL were taken each 0.25 h in the first hour, each 0.5 h in the second hour, and then each hour; subsequently, the same amount was replaced by fresh PBS to keep the total volume constant. Each aliquot was centrifuged at 5500 rpm for 10 min, and its absorbance was collected at 247 nm to calculate the cumulative release (CR) of amoxicillin in Cs-Al NDs according to

$$CR(\%) = \frac{m_{t=0} - m_{t=n}}{m_{t=0}} \times 100, \quad (2)$$

where  $m_{t=0}$  is the amoxicillin amount content in Cs-Al NDs at  $t = 0$  (g) and  $m_{t=n}$  is the amoxicillin amount contents in Cs-Al NDs at  $t = n$  (g).

## 2.6. In Vitro Cytotoxicity Assessment

**2.6.1. Human Cell Line Cultivation.** Human prostatic epithelial PWR-1E and Caucasian prostate adenocarcinoma PC-3 cell lines were cultured and incubated in a 96-well plate using Dulbecco's modified Eagle's medium (DMEM) at 37°C and under a 5%  $CO_2$ -humidified air atmosphere for 24 h. DMEM was supplemented with 10% fetal bovine serum, 1% penicillin-streptomycin, and keratinocyte cell culture medium. The keratinocyte cell culture medium was previously supplemented with 10% bovine pituitary extract and an EGF recombinant human protein. Cell lines were passaged up to 40 and proliferated until reaching 70-80% of confluency prior cultivation with Cs-Al NDs. After cultivation and incubation, DMEM was removed and replaced by freshly supplemented DMEM containing Cs-Al NDs at 10, 25, and 50  $\mu\text{g/mL}$  using PBS as the culture medium control in which the nanodisks were previously dispersed in the same PBS until reaching 200  $\mu\text{g/mL}$ . Cell lines were cultured and incubated under the same conditions for 48 and 72 h with triplicate.

**2.6.2. Trypan Blue and CellTiter 96® Aqueous Viability Assays.** The viability of PWR-1E and PC-3 cell lines was evaluated through 2 different methods, trypan blue and CellTiter 96® Aqueous. After cultivation and incubation, DMEM was removed and cell lines were washed several times with PBS to eliminate the residual Cs-Al NDs. For the first method, fresh DMEM and 10  $\mu\text{L}$  of trypan blue were added to each well following a volume ratio of 10:1, respectively. Cell lines were then incubated under the same conditions for 2 h. After incubation, cell lines were placed into a Neubauer chamber for manual cell counting to determine the cell viability (CV) per mL. After

counting the cells that excluded trypan blue, the CV was calculated according to

$$CV(\%) = \frac{\text{Cells that excluded dye}}{\text{Total cells}} \times 100. \quad (3)$$

The second method consisted in a colorimetry technique using a solution composed of (3-(4,5-dimethylthiazol-2-yl)-5-(3-carboxymethoxyphenyl)-2-(4-sulfophenyl)-2H-tetrazolium) MTS and phenazine ethosulfate (PES) as an electronic coupling agent. This assay was performed using a CellTiter 96® Aqueous One Solution Cell Proliferation kit, in which 20  $\mu\text{L}$  of the MTS/PES stable solution was added to the cell line culture wells and then allowed to incubate at 37°C for 2 h. The cell viability was evaluated using Multiskan FC Microplate Photometer by Thermo Fisher Scientific, where the absorbance was measured at 490 nm to determine the total number of viable cells in a culture in which the absorbance value was directly proportional to this total number.

**2.7. Statistical Analysis.** The statistical analysis was investigated by a one-way analysis of variance (ANOVA) to determine the significance level of  $p < 0.05$ . GraphPad Prism v6.0 program was used to analyze the experimental data that was performed in triplicate and expressed as the mean  $\pm$  standard deviation.

## 3. Results and Discussion

**3.1. Characterization of Cs-Al NDs.** Scanning electron microscopy (SEM) images shown in Figures 1(a) and 1(b) determine the morphological features of the as-synthesized Cs-Al NDs. Agglomeration can be observed since the nanodisks were lyophilized previously, but the shape of the disks can still be seen clearly as shown in the SEM image in Figure 1(b) [19]. The nanoparticles were successfully synthesized with a more disk shape than the usual spherical or common structures, presenting a regular and smooth surface but a wide size range, which can be attributed to many factors such as the biopolymer concentrations and electrostatic interaction that occurs during ionotropic gelation using sodium tripolyphosphate (STPP) as a highly charged compound [20, 21]. The combination of chitosan and alginate leads the spontaneous aggregation and formation of polyion complexes through the interaction of the carboxyl and amine groups within the structure of both polymers, respectively [22]. Additionally, the electrostatic interaction helps with the formation of polyelectrolyte complexes by using a cross-linking agent such as STPP, which contributes to the cross-linking and orientation of the nanoparticles during the growth [23–25]. Some reports have shown that the variation of several parameters such as the concentration and weight ratio of chitosan and alginate, as well as the pH solution and addition order, can significantly affect the size and shape of the final nanoparticle and even the structure that may be either heterogeneous or homogenous [22]. Wasupalli and Verma found that a balance between pH solution and strong electrostatic interaction leads to the formation of nanofibers, whereas with a weaker interaction it tends to form

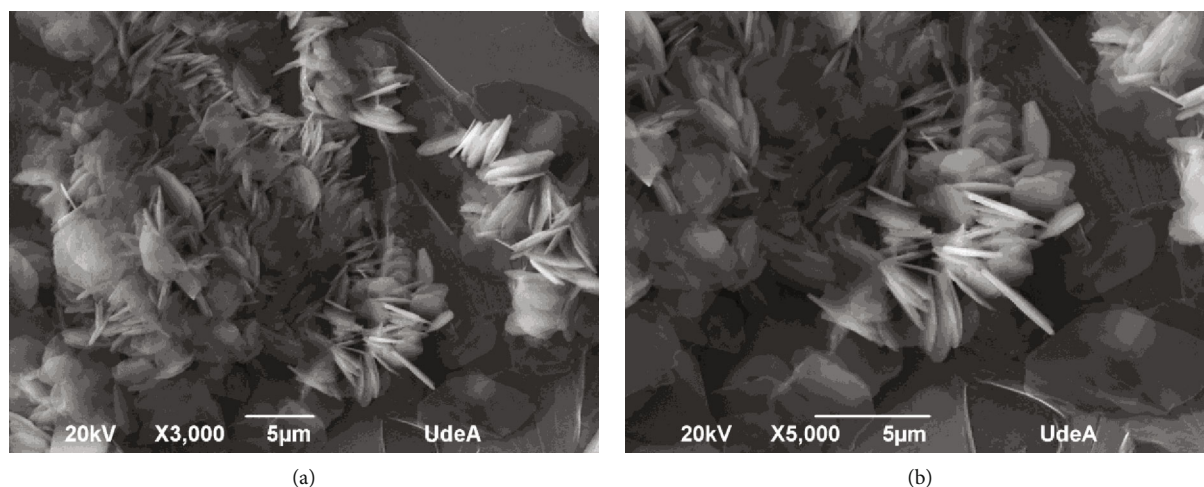


FIGURE 1: Scanning electron microscopy (SEM) images of the as-synthesized Cs-Al NDs at (a)  $\times 3,000$  and (b)  $\times 5,000$  magnifications.

nanocolloids [22]. Other reports made by Jeddi and Mahkam and Nalini et al. showed the formation of nanorods using chitosan, alginate, and a highly charged agent, which confirms that a strong electrostatic interaction is working as crosslinking between polymers, which is in agreement with the results obtained in this study [26, 27]. Besides, the presence of dense and agglomerated Cs-Al NDs in Figure 1(a) can be easily related to the availability of amine and carboxylic functional groups that produced strong electrostatic interaction on the surface [28]. This behaviour can be also observed in the size particle distribution as shown in Figure 2.

The chitosan/alginate weight ratio and pH of the solution in which nanodisks are dispersed play an important role in physical properties such as hydrodynamic size, agglomeration, and polydispersity [29]. According to the histograms, the particle size distribution is influenced by the pH of PBS solutions, indicating different responses in acidic and basic mediums. The particle size of Cs-Al NDs increases significantly at pH 1.2 as shown in Figure 2(a), obtaining a hydrodynamic average diameter of  $227 \pm 100$  nm, which can be related to the collapse of the chitosan molecule structure due to deprotonation of amine functional groups on the surface and also to the formation of intermolecular hydrogen bonding during the gelation process [30]. Compared to the hydrodynamic average diameter for Cs-Al NDs in PBS solution at pH 7.4, a decrease up to  $152 \pm 67$  nm is observed in Figure 2(b), indicating good stability at neutral pH. The presence of potassium ions from the STPP appears to be a very important factor in the formation of nanodisk shapes, leading the rapid increase in the agglomeration and particle size produced by a compact membrane of chitosan on the surface of the nanodisks [31, 32]. These results of particle size distribution and hydrodynamic size are consistent with the SEM images reported above and are in agreement with the results reported in the literature about the synthesis of chitosan/alginate nanoparticles by ionotropic gelation [6, 33].

Information related to the chemical structure of the Cs-Al NDs prepared using STTP as ionotropic gelation agent is shown in Figure 3. The spectrum shows the specimens in which vibrations for different functional groups were identi-

fied. The broadband between  $3370$  and  $2950\text{ cm}^{-1}$  corresponds to the N-H and O-H stretching vibrations, representing the aliphatic primary amine and alcohol groups, respectively [34, 35]. The peak at  $2874\text{ cm}^{-1}$  confirmed the presence of aliphatic C-H stretching [36, 37]. The deformation of N-acetylglucosamine determines the possible interaction between the amine and phosphate groups in the Cs-Al NDs, which can be evidenced by the presence of the peaks around  $1592$  and  $1529\text{ cm}^{-1}$ , as well as the peak at  $1407\text{ cm}^{-1}$  indicating an antisymmetric deformation of methyl groups due to the electrostatic interaction with STTP [37–39]. The presence of alginate can be evidenced by the stretching vibration of carboxylic acid at  $1382$ ,  $1214$ , and  $1027\text{ cm}^{-1}$  [36, 40]. The peak at  $1306$ ,  $1129$ ,  $1065$ , and  $891\text{ cm}^{-1}$  corresponded to the tertiary amide group, C-O-C glycosidic bond, C-O stretching vibration, and C-O-C stretching vibration [36, 37]. The wavenumber range between  $790$  and  $440\text{ cm}^{-1}$  is attributed to the electrostatic interaction between the functional groups of chitosan and STTP, which can be described as a derivation of linkages with N-H symmetric vibrations [38].

Crystallinity of the as-prepared Cs-Al NDs was evaluated by using the X-ray diffraction (XRD) technique. The diffraction pattern is shown in Figure 4, which evidenced the presence of characteristic peaks corresponding to the chitosan and alginate polymers. Peaks at  $9^\circ$  and  $19^\circ$  confirm the existence of chitosan within the nanodisks' structure and are attributed to the formation of hydrogen bonds between the amine and hydroxyl groups and the dilution of chitosan in acetic acid, respectively [23], whereas peak at  $12^\circ$  and also a broad peak starting at  $35^\circ$  correspond to the presence of alginate [14, 29, 41]. An intense peak was observed at  $23^\circ$  indicating the presence of the Cs-Al NDs, which can be inferred that alginate is influencing the crystalline properties of chitosan through hydrogen bonding, and electrostatic interaction between negative and positive charges, confirming the formation of a polyelectrolyte complex using the ionic gelation method [14, 23, 42]. These results are in agreement with those reported in the literature, allowing to state that the Cs-Al NDs present high crystallinity, strong electrostatic

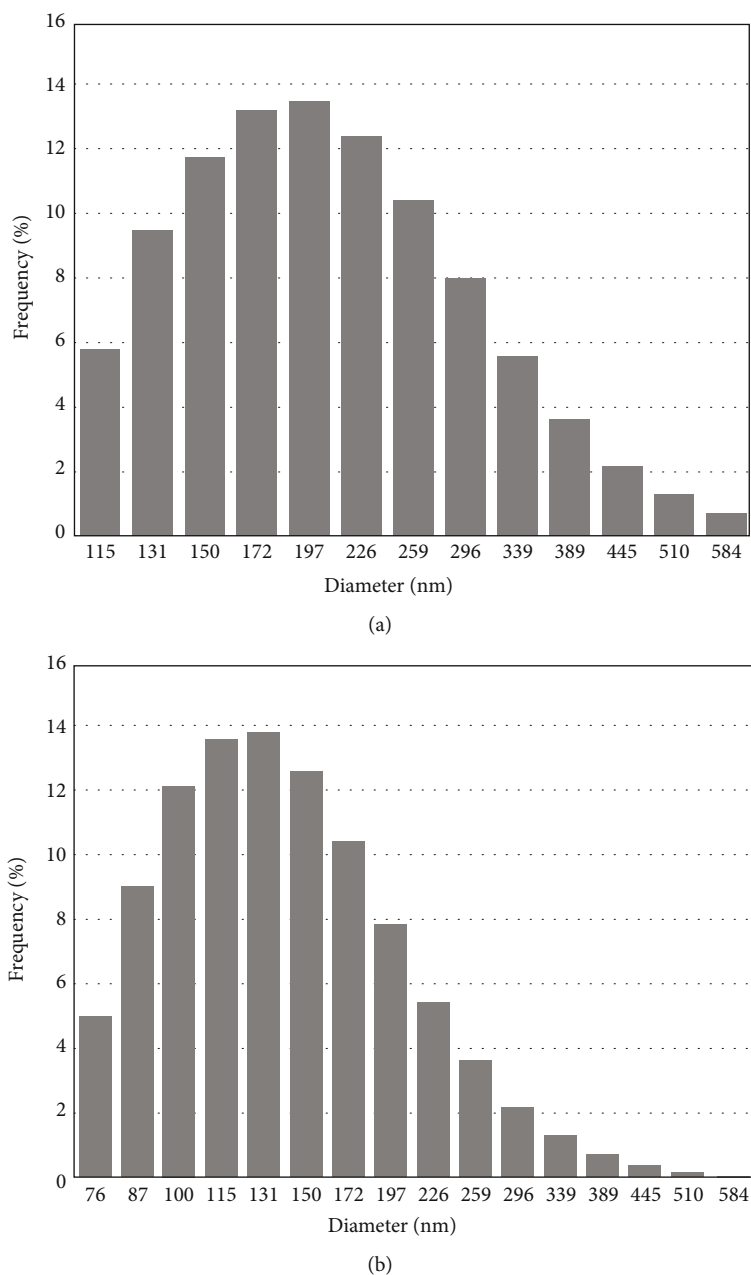


FIGURE 2: Particle size distribution of Cs-Al NDs in PBS at pH (a) 1.2 and (b) 7.4.

interaction, and good order of the crystallites [19]. The crystallite size for the Cs-Al NDs was calculated to be 1.6 nm from the peak with the strongest intensity at  $23^\circ$ , according to the following Debye-Scherrer equation (1):

$$d = \frac{k \times \lambda}{\beta \times \cos \theta}, \quad (4)$$

where  $d$  (nm) is the crystallite size,  $k$  (0.94) is the Scherrer constant,  $\lambda$  (Cu – K $\alpha$  = 0.1541 nm) is the X-ray wavelength,  $\beta$  (FWHM, rad) is the full width at half maximum, and  $\theta$  (rad) is the Bragg diffraction angle.

**3.2. Encapsulation Efficacy and In Vitro Drug Release.** The amoxicillin encapsulation efficiency in Cs-Al NDs was calculated from a supernatant by triplicate, giving an efficiency of  $74.98\% \pm 0.23$ . This result indicates that these nanodisks are a suitable material for a successful loading of amoxicillin and was consistent with the results reported in the literature of other chitosan/alginate nanoparticles [36, 40, 43]. The presence of the STPP crosslinking agent influences the encapsulation efficiency characteristic due to the formation of chitosan/alginate-TPP complex that produces an electrostatic interaction between carboxylic and amine functional groups of chitosan and amoxicillin, increasing the loading of amoxicillin in Cs-Al NDs [44]. However, the encapsulation efficiency is increasing in agglomeration after ionotropic

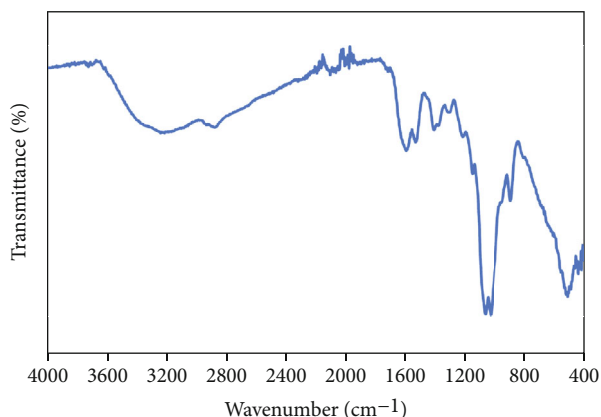


FIGURE 3: Fourier transform infrared (FTIR) spectrum of the as-synthesized Cs-Al NDs.

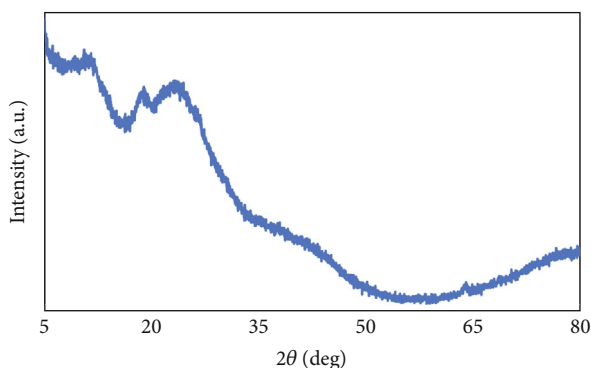


FIGURE 4: X-ray diffraction (XRD) pattern of the as-synthesized Cs-Al NDs.

gelation as shown in Figure 1, which is expected to decrease the surface area availability of the nanodisks, leading to the saturation of the polymer matrix during the drug loading [36, 45].

The *in vitro* release of amoxicillin from Cs-Al NDs was carried out in PBS solution at pH 1.2 and 7.4 and was monitored as a function of time as shown in Figure 5. According to the curves, the encapsulated drug release showed to be significantly high, which obtained a maximum release amount within 8 h of 63.2 and 52.3% at pH 1.2 and 7.4, respectively. There were two stages in the cumulative amoxicillin release of the Cs-Al NDs in both pH, where initially the release increased rapidly and constantly (burst effect) in the first 2 h due to the limited distribution of the drug onto the surface, and then during the following 6 h, the release slightly decreased and became more stable [46, 47]. Thereby, the release profile of amoxicillin encapsulated in Cs-Al NDs are shown to be sustainable, which is an important factor in reducing the hepatotoxicity effects and damage to healthy cells in anticancer drug delivery systems [27, 48].

Although similar results were observed for both pH condition, Cs-Al NDs at pH 7.4 best released the encapsulated drug within 8 h, suggesting that the Cs-Al NDs can be capable to hold and have controlled release capacity of amoxicillin. Hence, these results can be considered positive, since a

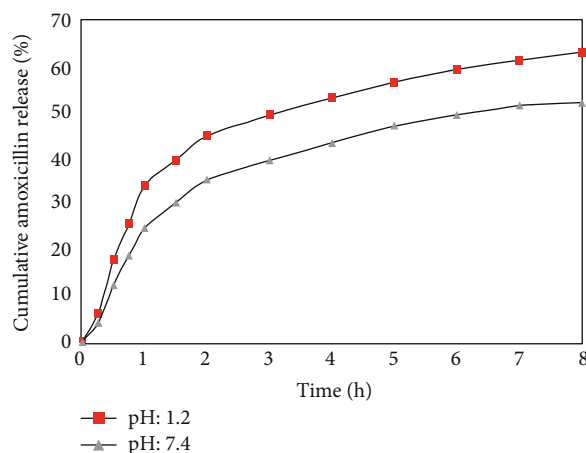


FIGURE 5: Amoxicillin release from Cs-Al NDs in PBS solutions with pH at 1.2 and 7.4.

long-term drug delivery system is more suitable for anticancer treatment, due to the low hepatotoxicity for controlled drug concentration, and less doses are required being an economic and therapeutic advantage [49]. This prolonged period and reduced dose at pH 7.4 may be attributed to the electrostatic interaction between functional groups of the chitosan/alginate-STPP complex and the drug, providing good pH sensitivity which improves the controlled release capacity of the Cs-Al NDs [50, 51]. On the contrary, the faster release found at pH 1.2 can be related to a higher solubility and swelling capability of Cs-Al NDs, since there was a change in the complex structure due to a possible protonation of the carboxylic and amine groups weakening the bonding with STPP and thus decreasing the  $\pi$ - $\pi$  interaction between amoxicillin and the Cs-Al NDs structure [51, 52]. According to the results, a partial release of amoxicillin was observed which may be attributed by the fact that the nanodisks had a low degradation during the test. However, a greater degradation of the polymer framework occurred for the nanodisks exposed to acidic pH, indicating the diffusion of amoxicillin due to the polymer chain relaxation, in which these results were in agreement with those reported in the literature [36, 53].

**3.3. In Vitro Cytotoxicity Assessment.** Trypan blue and Cell-Titer 96® AQueous tests were performed to evaluate cytotoxicity using different concentrations (10, 25, and 50  $\mu$ g/mL) of Cs-Al NDs against two cell lines, PWR-1E and PC-3. According to the results from both methods shown in Figures 6(a)–6(d) and 7(a)–7(d), no significant toxicity was observed in the cell lines providing a viability above 80%, which is in agreement with the cytotoxicity requirements for the application of biomaterials in drug delivery systems [50, 51]. Although the viability slightly decreased when the exposure concentration with Cs-Al NDs increases, as was observed mainly in Figures 7(a) and 7(c) for PWR-1E cells, the high percentage corresponds to no-cytotoxic effects indicating that no damage was caused to the cell membrane [2], allowing their normal growth due to the excellent biocompatibility of chitosan and alginate biopolymers [54].

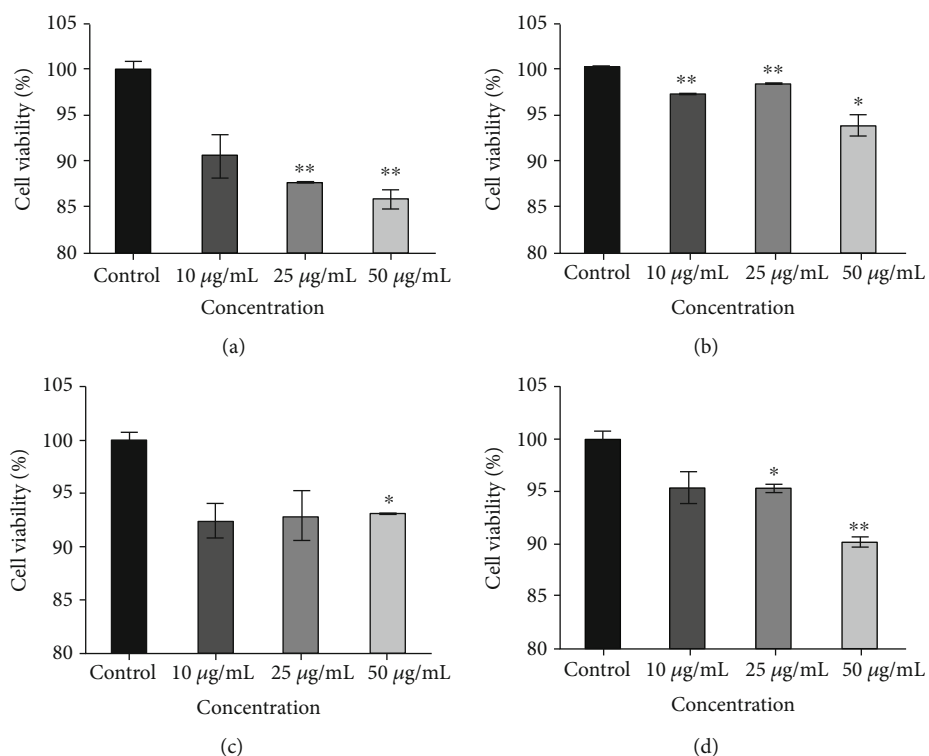


FIGURE 6: Cell viability using trypan blue technique of PWR-1E line after (a) 48 and (c) 72 h and PC-3 line after (b) 48 and (d) 72 h, exposed to Cs-Al NDs. Significant difference with control: \* $p < 0.05$  and \*\* $p < 0.01$ .

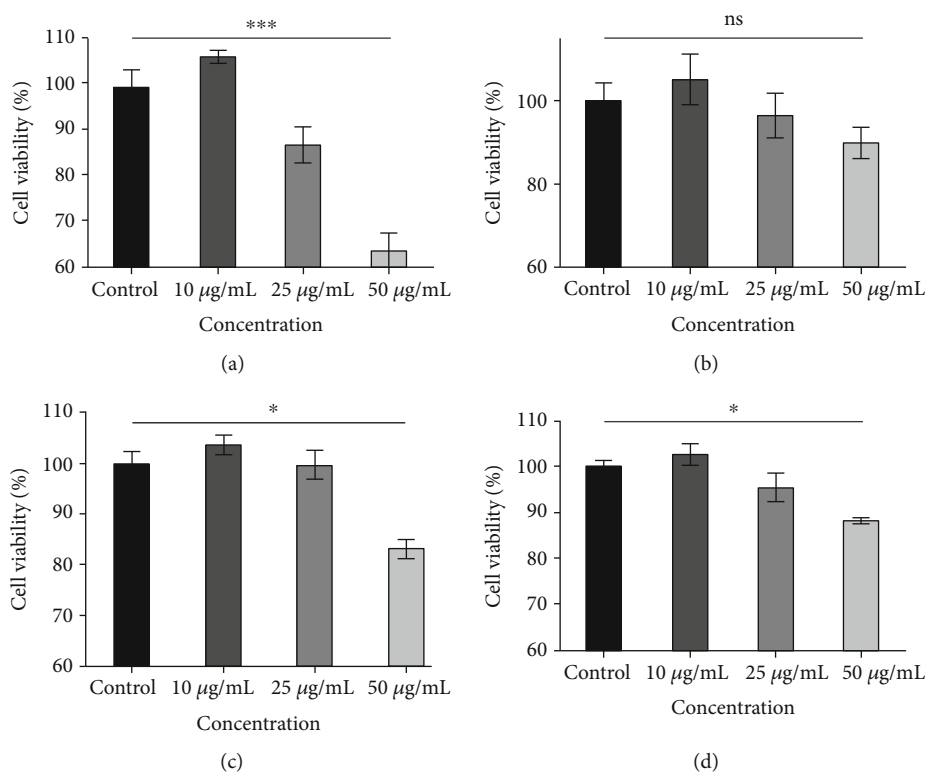


FIGURE 7: Cell viability using CellTiter 96® AQueous technique of PWR-1E line after (a) 48 and (c) 72 h and PC-3 line after (b) 48 and (d) 72 h, exposed to Cs-Al NDs. Significant difference with control: \* $p < 0.05$ , \*\* $p < 0.01$ , and \*\*\* $p < 0.001$ . ns = no significant difference.

Differences were observed between the normal cell line and the adenocarcinoma culture as shown in Figures 6 and 7, which can be inferred that the Cs-Al NDs provides better biocompatibility regarding the adenocarcinoma cells, considering them suitable for applications in cancer treatments as nanocarriers for the delivery of drugs. However, the cell viability tends to increase when exposed for 72 h, indicating that eventually cells keep growing due to an improvement in the biocompatibility, promoted as a positive characteristic in terms of prolonged drug delivery [21], which is the opposite for the case of adenocarcinoma cells. From the results, it is also important to take into account that increasing the Cs-Al NDs concentration may affect negatively the cell viability, as was observed for the treatment using 50  $\mu\text{g/mL}$  which resulted in a slight inhabitation of both cell lines due to induced oxidative stress on cells or changes in the cell membrane, as well as inducing damage of the DNA [1, 55, 56]. These results are in quantitative agreement with the results reported in the literature, which obtained low growth inhibition using similar nanomaterials synthesized with chitosan and alginate biopolymers for cytotoxicity assessment [13, 14, 57].

Although the results from trypan blue method indicated high cell viability compared to those obtained by using the CellTiter 96® AQueous method, reports show less accuracy using trypan blue. Accordingly, these results from the CellTiter 96® AQueous method are more reliable and the cytotoxicity pattern observed seems to be in agreement with other reports, in which higher concentration of nanoparticles is the main cause of inducing negative effects on the cell viability [58]. Among these reports, the use of alginate/chitosan and other types of nanocarriers against different cells lines was involved, and the results showed a similar trend in which a variation in the cell viability may be attributed to the selectivity with no discrimination toward the normal and cancerous cells [1, 36, 40, 59].

#### 4. Conclusions

We report a facile strategy to synthesize chitosan-alginate nanodisks (Cs-Al NDs) using ionotropic gelation method and sodium tripolyphosphate (STPP) as a highly charged agent. We observed the interaction between charges of the amine group of chitosan and the carboxyl group of alginate, which was promoted by degradation of some chemical structures and then the electrostatic interaction with phosphates, leading to the formation of the nanodisks as was reported in the SEM images. The characterization results corroborated that the Cs-Al NDs has a high and regular crystalline orientation due to the strong interaction between the polymers. We also found that the hydrodynamic size increases when the nanodisks are exposed to an acidic environment, in which a burst release of drug due to the swelling behaviour in pH 1.2 may occur. Therefore, in a basic environment, the nanodisk presents small hydrodynamic sizes, indicating a better and more controlled release of amoxicillin. These Cs-Al NDs showed high cell viability above 80% when exposed for 48 and 72 h, taking into account that the viability may

increase due to the high biocompatibility of the nanodisks, which represent an efficient nanomaterial for medical and pharmaceutical applications, and are also shown to be a new platform for further and deeper studies involving different drugs and cell lines, as well as *in vivo* tests.

#### Data Availability

The data used to support the findings of this study are included within the article.

#### Conflicts of Interest

The authors declare that there is no conflict of interest regarding the publication of this paper.

#### Acknowledgments

The authors are grateful to the Administrative Department of Science, Technology and Innovation (known in Spanish as Colciencias) for the financial support provided by the Young Researchers Program. This work made use of the Research, Innovation and Development of Materials Centre (known in Spanish as CIDEMAT), which is supported through the Microscopy Laboratory at the Universidad de Antioquia. The authors would like to acknowledge the support of the Universidad de Cartagena for the qualified human resource and facilities in the development of experiments. The authors would also like to thank the Doctorate in Engineering Program from the Universidad de Cartagena for their support with the doctoral training of David Patiño-Ruiz.

#### References

- [1] M. Bilal, T. Rasheed, H. M. N. Iqbal, C. Li, H. Hu, and X. Zhang, "Development of silver nanoparticles loaded chitosan-alginate constructs with biomedical potentialities," *International Journal of Biological Macromolecules*, vol. 105, Part 1, pp. 393–400, 2017.
- [2] D. Aluani, V. Tzankova, M. Kondeva-Burdina et al., "Evaluation of biocompatibility and antioxidant efficiency of chitosan-alginate nanoparticles loaded with quercetin," *International Journal of Biological Macromolecules*, vol. 103, pp. 771–782, 2017.
- [3] T. Wu, J. Huang, Y. Jiang et al., "Formation of hydrogels based on chitosan/alginate for the delivery of lysozyme and their antibacterial activity," *Food Chemistry*, vol. 240, pp. 361–369, 2018.
- [4] M. Gierszewska, J. Ostrowska-Czubenko, and E. Chrzanowska, "pH-responsive chitosan/alginate polyelectrolyte complex membranes reinforced by tripolyphosphate," *European Polymer Journal*, vol. 101, pp. 282–290, 2018.
- [5] M. He, X. Zhang, W. Yao, C. Wang, L. Shi, and P. Zhou, "Construction of alternate layered chitosan/alginate composite hydrogels and their properties," *Materials Letters*, vol. 200, pp. 43–46, 2017.
- [6] K. Ling, H. Wu, A. S. Neish, and J. A. Champion, "Alginate/chitosan microparticles for gastric passage and intestinal release of therapeutic protein nanoparticles," *Journal of Controlled Release*, vol. 295, pp. 174–186, 2019.

- [7] L. Zakaria, T. W. Wong, N. K. Anuar et al., "Enhancing sustained drug release property of chitosan in spheroids through crosslinking reaction and coacervation," *Powder Technology*, vol. 354, pp. 815–821, 2019.
- [8] W. Zhang, H. Wang, X. Hu et al., "Multicavity triethylenetetramine-chitosan/alginate composite beads for enhanced Cr(VI) removal," *Journal of Cleaner Production*, vol. 231, pp. 733–745, 2019.
- [9] F. N. Sorasitthiyankarn, P. Ratnatilaka Na Bhuket, C. Muangnoi, P. Rojsitthisak, and P. Rojsitthisak, "Chitosan/alginate nanoparticles as a promising carrier of novel curcumin diethyl diglutarate," *International Journal of Biological Macromolecules*, vol. 131, pp. 1125–1136, 2019.
- [10] M. Halimi, M. Alishahi, M. R. Abbaspour, M. Ghorbanpoor, and M. R. Tabandeh, "Valuable method for production of oral vaccine by using alginate and chitosan against *Lactococcus garvieae*/*Streptococcus iniae* in rainbow trout (*Oncorhynchus mykiss*)," *Fish & Shellfish Immunology*, vol. 90, pp. 431–439, 2019.
- [11] M. A. Khan, C. Yue, Z. Fang et al., "Alginate/chitosan-coated zein nanoparticles for the delivery of resveratrol," *Journal of Food Engineering*, vol. 258, pp. 45–53, 2019.
- [12] D. K. Bedade, Y. B. Sutar, and R. S. Singhal, "Chitosan coated calcium alginate beads for covalent immobilization of acrylamidase: process parameters and removal of acrylamide from coffee," *Food Chemistry*, vol. 275, pp. 95–104, 2019.
- [13] S. Wichai, P. Chuysinuan, S. Chairwut, P. Ekabutr, and P. Supaphol, "Development of bacterial cellulose/alginate/chitosan composites incorporating copper (II) sulfate as an antibacterial wound dressing," *Journal of Drug Delivery Science and Technology*, vol. 51, pp. 662–671, 2019.
- [14] J. Venkatesan, J. Y. Lee, D. S. Kang et al., "Antimicrobial and anticancer activities of porous chitosan-alginate biosynthesized silver nanoparticles," *International Journal of Biological Macromolecules*, vol. 98, pp. 515–525, 2017.
- [15] A. Da S Pereira, M. M. Diniz, G. De Jong et al., "Chitosan-alginate beads as encapsulating agents for *Yarrowia lipolytica* lipase: Morphological, physico-chemical and kinetic characteristics," *International Journal of Biological Macromolecules*, vol. 139, pp. 621–630, 2019.
- [16] F. Maestrelli, M. Jug, M. Cirri, I. Kosalec, and P. Mura, "Characterization and microbiological evaluation of chitosan-alginate microspheres for cefixime vaginal administration," *Carbohydrate Polymers*, vol. 192, pp. 176–183, 2018.
- [17] C. Qin, J. Zhou, Z. Zhang, W. Chen, Q. Hu, and Y. Wang, "Convenient one-step approach based on stimuli-responsive sol-gel transition properties to directly build chitosan-alginate core-shell beads," *Food Hydrocolloids*, vol. 87, pp. 253–259, 2019.
- [18] A. P. H. Barros, M. T. A. Morantes, M. I. C. Hoyos, and L. J. M. Ospino, "Preparación de nanopartículas de quitosano modificadas con alginato de sodio con potencial para la liberación controlada de medicamentos," *Revista EIA*, vol. 12, no. 57 5, pp. 75–83, 2016.
- [19] M. Ji, X. Sun, X. Guo et al., "Green synthesis, characterization and *in vitro* release of cinnamaldehyde/sodium alginate/chitosan nanoparticles," *Food Hydrocolloids*, vol. 90, pp. 515–522, 2019.
- [20] A. Bhattacharyya, D. Mukherjee, R. Mishra, and P. P. Kundu, "Preparation of polyurethane-alginate/chitosan core shell nanoparticles for the purpose of oral insulin delivery," *European Polymer Journal*, vol. 92, pp. 294–313, 2017.
- [21] K. Yoncheva, M. Merino, A. Shenol et al., "Optimization and in-vitro/in-vivo evaluation of doxorubicin-loaded chitosan-alginate nanoparticles using a melanoma mouse model," *International Journal of Pharmaceutics*, vol. 556, pp. 1–8, 2019.
- [22] G. K. Wasupalli and D. Verma, "Molecular interactions in self-assembled nano-structures of chitosan-sodium alginate based polyelectrolyte complexes," *International Journal of Biological Macromolecules*, vol. 114, pp. 10–17, 2018.
- [23] H. Wang, X. Gong, Y. Miao et al., "Preparation and characterization of multilayer films composed of chitosan, sodium alginate and carboxymethyl chitosan-ZnO nanoparticles," *Food Chemistry*, vol. 283, pp. 397–403, 2019.
- [24] R. Dubey, J. Bajpai, and A. K. Bajpai, "Chitosan-alginate nanoparticles (CANPs) as potential nanosorbent for removal of Hg (II) ions," *Environmental Nanotechnology, Monitoring & Management*, vol. 6, pp. 32–44, 2016.
- [25] T. Niaz, H. Nasir, S. Shabbir, A. Rehman, and M. Imran, "Poly-ionic hybrid nano-engineered systems comprising alginate and chitosan for antihypertensive therapeutics," *International Journal of Biological Macromolecules*, vol. 91, pp. 180–187, 2016.
- [26] M. K. Jeddi and M. Mahkam, "Magnetic nano carboxymethyl cellulose-alginate/chitosan hydrogel beads as biodegradable devices for controlled drug delivery," *International Journal of Biological Macromolecules*, vol. 135, pp. 829–838, 2019.
- [27] T. Nalini, S. K. Basha, A. M. Mohamed Sadiq, V. S. Kumari, and K. Kaviyarasu, "Development and characterization of alginate / chitosan nanoparticulate system for hydrophobic drug encapsulation," *Journal of Drug Delivery Science and Technology*, vol. 52, pp. 65–72, 2019.
- [28] F. M. Goycoolea, G. Lollo, C. Remuñán-López, F. Quaglia, and M. J. Alonso, "Chitosan-alginate blended nanoparticles as carriers for the transmucosal delivery of macromolecules," *Biomacromolecules*, vol. 10, no. 7, pp. 1736–1743, 2009.
- [29] S. Maity, P. Mukhopadhyay, P. P. Kundu, and A. S. Chakraborti, "Alginate coated chitosan core-shell nanoparticles for efficient oral delivery of naringenin in diabetic animals—an in vitro and in vivo approach," *Carbohydrate Polymers*, vol. 170, pp. 124–132, 2017.
- [30] T. Cerchiara, A. Abruzzo, M. di Cagno et al., "Chitosan based micro- and nanoparticles for colon-targeted delivery of vancomycin prepared by alternative processing methods," *European Journal of Pharmaceutics and Biopharmaceutics*, vol. 92, pp. 112–119, 2015.
- [31] S. Abdelghany, M. Alkhaldeh, and H. S. Alkhatib, "Carra-geenan-stabilized chitosan alginate nanoparticles loaded with ethionamide for the treatment of tuberculosis," *Journal of Drug Delivery Science and Technology*, vol. 39, pp. 442–449, 2017.
- [32] S. Bhunchu, P. Rojsitthisak, and P. Rojsitthisak, "Effects of preparation parameters on the characteristics of chitosan-alginate nanoparticles containing curcumin diethyl disuccinate," *Journal of Drug Delivery Science and Technology*, vol. 28, pp. 64–72, 2015.
- [33] J. Liu, J. Xiao, F. Li, Y. Shi, D. Li, and Q. Huang, "Chitosan-sodium alginate nanoparticle as a delivery system for  $\epsilon$ -polylysine: preparation, characterization and antimicrobial activity," *Food Control*, vol. 91, pp. 302–310, 2018.
- [34] A. Sharma, K. Sood, J. Kaur, and M. Khatri, "Agrochemical loaded biocompatible chitosan nanoparticles for insect pest management," *Biocatalysis and Agricultural Biotechnology*, vol. 18, p. 101079, 2019.

- [35] R. R. Gadkari, S. Suwalka, M. R. Yogi, W. Ali, A. Das, and R. Alagirusamy, "Green synthesis of chitosan-cinnamaldehyde cross-linked nanoparticles: Characterization and antibacterial activity," *Carbohydrate Polymers*, vol. 226, article 115298, 2019.
- [36] F. N. Sorasitthyanukarn, C. Muangnoi, P. Ratnatilaka Na Bhuket, P. Rojsitthisak, and P. Rojsitthisak, "Chitosan/alginate nanoparticles as a promising approach for oral delivery of curcumin diglutamic acid for cancer treatment," *Materials Science and Engineering: C*, vol. 93, pp. 178–190, 2018.
- [37] V. S. Gondil, T. Dube, J. J. Panda, R. M. Yennemalli, K. Harjai, and S. Chhibber, "Comprehensive evaluation of chitosan nanoparticle based phage lysis delivery system; a novel approach to counter *S. pneumoniae* infections," *International Journal of Pharmaceutics*, 2019.
- [38] S. F. Hosseini, M. R. Soleimani, and M. Nikkhal, "Chitosan/sodium tripolyphosphate nanoparticles as efficient vehicles for antioxidant peptidic fraction from common kilka," *International Journal of Biological Macromolecules*, vol. 111, pp. 730–737, 2018.
- [39] Z. Sang, J. Qian, J. Han et al., "Comparison of three water-soluble polyphosphate tripolyphosphate, phytic acid, and sodium hexametaphosphate as crosslinking agents in chitosan nanoparticle formulation," *Carbohydrate Polymers*, vol. 230, p. 115577, 2020.
- [40] J. G. Rosch, H. Winter, A. N. DuRoss, G. Sahay, and C. Sun, "Inverse-Micelle Synthesis of Doxorubicin-Loaded Alginate-Chitosan Nanoparticles and *In Vitro* Assessment of Breast Cancer Cytotoxicity," *Colloid and Interface Science Communications*, vol. 28, pp. 69–74, 2019.
- [41] P. Mukhopadhyay, S. Maity, S. Mandal, A. S. Chakraborti, A. K. Prajapati, and P. P. Kundu, "Preparation, characterization and *in vivo* evaluation of pH sensitive, safe quercetin-succinylated chitosan-alginate core-shell-corona nanoparticle for diabetes treatment," *Carbohydrate Polymers*, vol. 182, pp. 42–51, 2018.
- [42] C. P. Gong, Y. Luo, and Y. Y. Pan, "Novel synthesized zinc oxide nanoparticles loaded alginate-chitosan biofilm to enhanced wound site activity and anti-septic abilities for the management of complicated abdominal wound dehiscence," *Journal of Photochemistry and Photobiology B: Biology*, vol. 192, pp. 124–130, 2019.
- [43] S. Arora, S. Gupta, R. K. Narang, and R. D. Budhiraja, "Amoxicillin loaded chitosan-alginate polyelectrolyte complex nanoparticles as mucopenetrating delivery system for *H. pylori*," *Scientia Pharmaceutica*, vol. 79, no. 3, pp. 673–694, 2011.
- [44] J. O. Akolade, H. O. B. Oloyede, M. O. Salawu, A. O. Amuzat, A. I. Ganiyu, and P. C. Onyenekwe, "Influence of formulation parameters on encapsulation and release characteristics of curcumin loaded in chitosan-based drug delivery carriers," *Journal of Drug Delivery Science and Technology*, vol. 45, pp. 11–19, 2018.
- [45] M. Xie, F. Zhang, H. Peng et al., "Layer-by-layer modification of magnetic graphene oxide by chitosan and sodium alginate with enhanced dispersibility for targeted drug delivery and photothermal therapy," *Colloids and Surfaces B: Biointerfaces*, vol. 176, pp. 462–470, 2019.
- [46] F. Shamekhi, E. Tamjid, and K. Khajeh, "Development of chitosan coated calcium-alginate nanocapsules for oral delivery of liraglutide to diabetic patients," *International Journal of Biological Macromolecules*, vol. 120, Part A, pp. 460–467, 2018.
- [47] X. Chen, M. Fan, H. Tan et al., "Magnetic and self-healing chitosan-alginate hydrogel encapsulated gelatin microspheres via covalent cross-linking for drug delivery," *Materials Science and Engineering: C*, vol. 101, pp. 619–629, 2019.
- [48] J. R. Lakkakula, T. Matshaya, and R. W. M. Krause, "Cationic cyclodextrin/alginate chitosan nanoflowers as 5-fluorouracil drug delivery system," *Materials Science and Engineering: C*, vol. 70, Part 1, pp. 169–177, 2017.
- [49] J. M. Unagolla and A. C. Jayasuriya, "Drug transport mechanisms and *in vitro* release kinetics of vancomycin encapsulated chitosan-alginate polyelectrolyte microparticles as a controlled drug delivery system," *European Journal of Pharmaceutical Sciences*, vol. 114, pp. 199–209, 2018.
- [50] Y. G. Bi, Z.-t. Lin, and S.-t. Deng, "Fabrication and characterization of hydroxyapatite/sodium alginate/chitosan composite microspheres for drug delivery and bone tissue engineering," *Materials Science and Engineering: C*, vol. 100, pp. 576–583, 2019.
- [51] K. Chen, Y. Ling, C. Cao, X. Li, X. Chen, and X. Wang, "Chitosan derivatives/reduced graphene oxide/alginate beads for small-molecule drug delivery," *Materials Science and Engineering: C*, vol. 69, pp. 1222–1228, 2016.
- [52] M. Kilicarslan, M. Ilhan, O. Inal, and K. Orhan, "Preparation and evaluation of clindamycin phosphate loaded chitosan/alginate polyelectrolyte complex film as mucoadhesive drug delivery system for periodontal therapy," *European Journal of Pharmaceutical Sciences*, vol. 123, pp. 441–451, 2018.
- [53] K. K. Patel, M. Tripathi, N. Pandey et al., "Alginate lyase immobilized chitosan nanoparticles of ciprofloxacin for the improved antimicrobial activity against the biofilm associated mucoid *P. aeruginosa* infection in cystic fibrosis," *International Journal of Pharmaceutics*, vol. 563, pp. 30–42, 2019.
- [54] X. Lv, W. Zhang, Y. Liu, Y. Zhao, J. Zhang, and M. Hou, "Hygroscopicity modulation of hydrogels based on carboxymethyl chitosan/Alginate polyelectrolyte complexes and its application as pH-sensitive delivery system," *Carbohydrate Polymers*, vol. 198, pp. 86–93, 2018.
- [55] X. Lv, Y. Liu, S. Song et al., "Influence of chitosan oligosaccharide on the gelling and wound healing properties of injectable hydrogels based on carboxymethyl chitosan/alginate polyelectrolyte complexes," *Carbohydrate Polymers*, vol. 205, pp. 312–321, 2019.
- [56] J. O. Adeyemi, E. E. Elemike, D. C. Onwudiwe, and M. Singh, "Bio-inspired synthesis and cytotoxic evaluation of silver-gold bimetallic nanoparticles using Kei-Apple (*Dovyalis caffra*) fruits," *Inorg. Chem. Commun.*, vol. 109, article 107569, 2019.
- [57] M. Almada, B. H. Leal-Martínez, N. Hassan et al., "Photothermal conversion efficiency and cytotoxic effect of gold nanorods stabilized with chitosan, alginate and poly(vinyl alcohol)," *Materials Science and Engineering: C*, vol. 77, pp. 583–593, 2017.
- [58] T. P. Mofokeng, M. J. Moloto, P. M. Shumbula, and P. Tetyana, "Synthesis, characterization and cytotoxicity of alanine-capped CuS nanoparticles using human cervical carcinoma HeLa cells," *Analytical Biochemistry*, vol. 580, pp. 36–41, 2019.
- [59] D. K. Chelike, A. Alagumalai, J. Acharya et al., "Functionalized iron oxide nanoparticles conjugate of multi-anchored Schiff's base inorganic heterocyclic pendant groups: Cytotoxicity studies," *Applied Surface Science*, vol. 501, article 143963, 2020.

